A critical examination of the residual cloud contamination and diurnal sampling effects on MODIS estimates of aerosol over ocean

Y. J. Kaufman, L. A. Remer, D. Tanré, R.-R. Li, R. Kleidman, S. Mattoo, R. Levy, T. F. Eck, B.N. Holben, C. Ichoku, V. Martins and I. Koren

ABSTRACT

Observations of the aerosol optical thickness (AOT) by the MODIS instruments aboard Terra and Aqua satellites are being used extensively for applications to climate and air quality studies. Data quality is essential for these studies. Here we add to the published MODIS validations by investigating the effects of unresolved clouds on the MODIS measurements of the AOT. The main cloud effect is from residual cirrus that increases the measured AOT by 0.015±0.003 at 0.55 μm. In addition, lower level clouds can add contamination. We examine the effect of lower clouds using the difference between simultaneously measured MODIS and AERONET AOT. The difference is positively correlated with the cloud fraction. However, interpretation of this difference is sensitive to the definition of cloud contamination vs. aerosol growth. If we consider this consistent difference between MODIS and AERONET to be entirely due to cloud contamination we get a total cloud contamination, of 0.025±0.005, though a more likely estimate is closer to 0.020 after accounting for aerosol growth issues. This reduces the difference between MODIS observed global aerosol optical thickness over the oceans and model simulations by half, from 0.04 to 0.02. However it is insignificant for studies of aerosol cloud interaction. We also examined how representative are the MODIS data of the diurnal average aerosol. Comparison to monthly averaged sunphotometer data confirms that either the Terra or Aqua estimate of global AOT is a valid representation of the daily average. Though in the vicinity of aerosol sources such as fires we do not expect this to be true.

1. Introduction

Two MODerate Imaging Spectrometers (MODIS [1]) were launched into polar orbit: aboard the Terra satellite in Dec. 1999 and the Aqua satellite in 2002. One of their primary missions is to observe the global aerosol system and its impact on climate and air quality. MODIS reports aerosol data at 10 km resolution, which is further aggregated to provide more condensed global data products at 1° resolution [2]. Surveys using Internet-based search engines show that MODIS aerosol data were used in at least 28 papers published in 2004, alone. They show that MODIS data are used for:

- Descriptions of the regional, seasonal and global distribution of aerosols, and their relationship to other pollutants [3-15],
- Studies of the effect of aerosol on atmospheric chemistry and local air pollution [16-18],
- Measurements of the aerosol effect on distribution of solar radiation and consequent radiative forcing of climate [19-24],
- Regional aerosol characterization[25-28], and

- Studies of the aerosol interaction with the meteorological field and with clouds [29-30],

Each application has different requirements for data availability, and for absolute and relative accuracy. In this paper we shall concentrate on examination of the MODIS aerosol data over oceans. Extensive comparison of these data against ground-based measurements by the sunphotometers of the AErosol Robotic NETwork (AERONET [31]) [2,32], have been used to quantify and validate the MODIS aerosol data quality. They concluded that MODIS aerosol data over the ocean meet the expected accuracy [33], meaning that retrieved AOT errors are $\Delta\tau=\pm0.03\pm0.05\tau$, where τ is the aerosol optical thickness (AOT). Slightly higher errors were found for dust [34]. Since the MODIS-observed multi-year global averaged AOT over the ocean [35] is about $\tau\sim0.13$, an error of ±0.03 may be quite significant.

In this paper we critically examine the MODIS aerosol data over oceans, looking for cloud contamination and diurnal sampling issues that may create biases in applications based on the long-term statistics from MODIS aerosol products. First we review the MODIS aerosol products in section 2 and validation in section 3. Then, we study what portion of this uncertainty is a bias due to contamination by cirrus clouds (section 4), or due to lower level clouds (sections 5). Section 6 discusses how a relationship between cloud and aerosol retrievals could either be physically real or an artifact. We end with an analysis of how representative the MODIS data are of the daily averaged aerosol (section 7).

2. The MODIS aerosol product

Above the oceans, the aerosol algorithm [33] derives the aerosol optical thickness and aerosol size distribution from MODIS spectral reflectance data, at a nominal resolution of 10 km (at nadir). Within this 10 km resolution, there are 400 MODIS data pixels at 0.5 km resolution, insuring good statistical representation of the 10 x 10 km^2 box. Aerosol products are retrieved providing that the target is at least 40° off the sunglint angle, and the scene is sufficiently free of clouds and surface inhomogeneities. Cloud screening is applied using combinations of spatial variability [37] tests in the visible channels and cirrus detection using the cirrus channel at 1.38 μm [38]. The spatial variability mask also eliminates data points that are adjacent to the clouds. On average the fraction of data points being eliminated by the screening mechanism is 80% higher than the fraction of cloudy pixels being analyzed in the cloud products [39]. The pixels remaining after cloud screening are used to derive the aerosol properties. Requiring a minimum of 10 cloud free pixels, the average of the 25^{th} to 75^{th} percentile (sorted by reflectance) of these pixels is assumed to be representative of the average cloud free conditions. This average is a robust value that was expected to completely eliminate residual contamination by clouds and cloud shadows which may have remained after the cloud screening and occupy an area less than 25% of the 10 km grid box.

3. MODIS aerosol validation

First we shall review the MODIS validation studies and their relevance to understanding

measurement bias and errors. The MODIS aerosol data are compared against measurements from the surface based AERONET. Over each AERONET site, averages are calculated, such that the AERONET data are averaged in time (±30 minutes) and MODIS data are averaged in space (±25km) [40]. This range of the MODIS spatial coverage and the AERONET temporal coverage was chosen as to minimize aerosol variability [41], and to maximize data availability in the presence of clouds. Winds that can shift the aerosol across the validation grid box generate a coupling between the aerosol spatial and temporal variability. Winds of 5-10 m/s during the 1 hour of AERONET measurements shift the aerosol by 20-40 km.

AERONET has about 200 locations around the world that measure the spectral extinction of direct sunlight and spectral-angular properties of scattered sky radiances. Together they provide estimates of the spectral AOT as well as aerosol size distribution and optical properties. The coverage is best over continental Europe and North America, and less dense over the oceans, due to the need for either islands or sea-shores for instrument installation. However, given the now, nearly five years of both MODIS and AERONET observations, there are enough co-located measurements to understand the statistics of the validation efforts [32,42].

A valid comparison is considered when AERONET reports at least 2 values (out of the possible 4-5 measurements) during the hour and MODIS reports at least 5 measurements (over the ocean segment of the 25 measurements) in the grid box of 50 km. The AERONET data accuracy [43] is $\Delta\tau=\pm 0.015$ at airmass= 1, where airmass is cosine of the solar zenith angle. For all latitudes and seasons the uncertainty is reduced to 0.01.

This validation protocol requires that both MODIS and AERONET data are observed under sufficiently clear conditions, meaning that MODIS validation is biased toward low cloudiness conditions. In fact, we found that the cloud fraction over the ocean, averaged over the entire validation data set is 30%, which is about half the average cloud fraction otherwise observed by MODIS. We note that the cloud fraction is defined here as the fraction of the pixels that were rejected from analysis by the aerosol algorithm. For a broken cloud field it is larger than the actual cloud fraction since cloud free pixels adjacent to the cloud are also rejected. This clear-sky bias to the validation set may imply biases to estimates of global AOT and other aerosol properties.

Is it possible, despite the rigorous cloud screening and the 25^{th} to 75^{th} percentile selection of data, that some cloud interference will remain in the aerosol data? There are two main possible sources of cloud contamination:

- high concentrations of broken cloudiness may generate illumination of the aerosol field beyond the 500 m distance from the clouds [44]; and
- although the cirrus correction eliminates cirrus cloud contamination above a threshold in cirrus reflectance at 1.38 μm of 0.01, some residual cirrus contamination may remain. The threshold of 0.01 is used in order to avoid false elimination of high altitude dust and to allow for sensor noise [38].

4. Residual thin cirrus contamination

To study the residual cirrus contamination, we divided the world into 13 geographic zones [35]: 12 zones are the products of 3 latitude regions (30°-60°N; 0-30°N; 0-30°S) and 4 longitude belts (0-90°E; 90°-180°E; 0-90°W; 90°-180°W), the 13th is the southern latitude belt (30°-60°S). For each zone, a scatter plot was generated that plotted the AOT as a function of the cirrus reflection at 1.38 μm calculated from the cirrus channel [45] (see Fig 1b for an example). Each point in the scatter plots represents a grid box of 10 km. The average AOT is computed as a function of a given range of cirrus reflectance (i.e. first point is the average AOT for cirrus reflectance of 0-0.001, second for 0.001-0.002 etc.). Cirrus contamination is measured as the elevation of the AOT above its value for the lowest cirrus reflectance interval.

Assuming that there is no physical relationship between the AOT and cirrus reflectance, the systematic relationship between the AOT and cirrus indicates cirrus contamination. The process is repeated for every zone (ocean only) for the first 9 months of 2004. The results are plotted in Fig. 2. Every point represents the results of the analysis of Fig. 1 for one zone and one month. There is a significant variation among the zones. The variation can result from poor statistics, mainly in zones with small ocean cover, and meteorological coincidental correlation between the cirrus clouds and aerosols. It can also result from the cirrus channel detection of high altitude dust in some of the zones. Dust located at 3-5 km, with little water vapor (<1 cm) left above it will influence the cirrus observations. Therefore to summarize the results, we combine two techniques. One is a simple average (dashed line) over the 13 zones and the second is average of the 25th to 75th percentile among the 13 zones (solid line), and to avoid these possible coincidental correlations between cirrus and aerosol. The second method eliminates fluctuations that can be caused by errors in extreme zones in specific months. The difference between the two methods of average calculations is small, meaning that the average is robust. Using the second analysis as the bench mark, we estimate the average cirrus contamination of:

$$\Delta\tau=0.012\pm0.0005 \quad \text{for Terra and} \quad \Delta\tau=0.018\pm0.002 \quad \text{for Aqua.} \qquad (1)$$

The errors in Eq. 1 represent standard error due to variability among the 12 months for Terra and Aqua separately. The difference between the two satellites is larger and may result from small differences in their respective calibration.

The cirrus contamination in eq. 1 was derived assuming that there is no interaction between the aerosol and the cirrus cloud and that any coincidental correlation will affect only some of the zones and will be cancel out in the 25th to 75th percentile average. In fact since meteorological influence is expected to vary from month to month, the small standard error in Eq 1 reflects their residual influence.. To tes the analysis further we repeated the calculations of the cirrus contamination using only regions in the tropical Pacific (30°S to 30°N, 90W to 90E) and the Southern Ocean (30S-60S) where most of the aerosol is low level oceanic aerosol, less likely to interact with the cirrus. The results for Terra are that the cirrus contamination is $\Delta\tau=0.011$ for the Pacific Ocean and $\Delta\tau=0.012$ once the Southern Ocean was included, basically same as the bulk analysis.

5. Contamination by clouds and cloud illumination

Broken clouds within or adjacent to the satellite field of view also may contaminate retrievals of aerosol properties. As cloud fraction increases within the scene, the potential for contamination increases. In Fig 3, we plot the MODIS AOT, the AERONET AOT and the difference between them, as a function of the cloud fraction determined by MODIS in the 50 km grid box centered on the AERONET station. AERONET sunphotometers derive the AOT by observing the attenuation of sunlight through the atmosphere. Sunlight is 3-6 orders of magnitude brighter than the sky or clouds and therefore cloud illumination cannot affect the AERONET AOTs. AERONET also has an independent cloud screening [46]. Though AERONET also may not be able to screen out very thin cirrus, the cirrus crystals strong forward scattering of diffuse light into the AERONET sunphotometer field of view results in only ~50% of the cirrus optical depth being translated into an increase in apparent optical thickness [47].

Figure 3 shows a correlation between MODIS AOT "error" and cloud fraction as defined by the MODIS aerosol algorithm. We note that this cloud fraction will always overestimate the true cloud fraction because the MODIS algorithm rejects both cloudy pixels and also those pixels adjacent to clouds. Thus, the global mean cloud fraction of ~60% corresponds in Figure 3 to cloud fraction of ~80%, where the corresponding difference between MODIS and AERONET is 0.010±0.002 and 0.025±0.005 for Terra and Aqua respectively. Some of the discrepancy between MODIS and AERONET at high cloud fractions is due to different treatment of cirrus contamination discussed in Section 4 and quantified in Eq. 1. Though AERONET may have similar difficulties as MODIS to screen out thin cirrus, AERONET measurements are not affected as much by the presence of thin cirrus clouds; while the MODIS field of view is ~0.1° AERONET field of view is 1.2° allowing half of the scattering by the thin cirrus clouds to be detected still in the field of view. Therefore we can expect AERONET to be affected only by 50% of the cirrus scattering and therefore only about half of the values in Eq. 1 (0.006 for Terra and 0.009 for Aqua) contribute to the discrepancy between MODIS and AERONET in Fig. 3. Thus, non-cirrus effects, associated with clouds, are contributing to elevating the global MODIS AOT retrievals by 0.004±0.002 for Terra and 0.016±0.005 for Aqua.

What is the origin of the cloud fraction dependence of the difference of MODIS vs AERONET? One possibility is that when cloud fraction is high over ocean there is a gradient from land, where the sunphotometer is located to the ocean with different meteorological conditions. To investigate this possibility we analyzed separately the difference between MODIS and AERONET for island stations only. There is no significant difference between the results, decreasing the probability that a systematic gradient, in cloudiness and aerosol conditions is the reason.

Another possibility to explain Fig. 3 is that despite our best efforts cloudy pixels are escaping our cloud mask and are being retrieved as aerosol. A third possibility related to the second is that clouds are brightening their surrounding pixels, even beyond the one pixel border that the MODIS algorithm imposes on the cloud mask. Cloud droplets are orders of magnitude larger than aerosol particles. Light scattering by large cloud droplets will be spectrally neutral. Therefore cloud-contaminated retrieved spectral optical

thickness will have less spectral dependence and be more neutral. We measure spectral dependence with the Angstrom Exponent (α), which defines the slope of ln(AOT) plotted against ln(wavelength). A larger α corresponds to a steeper slope, a greater spectral dependence and smaller particles. Thus, if cloud contamination is responsible for the differences in AOT between MODIS and AERONET in Fig. 3, then we expect two things: (1) as cloud fraction increases MODIS α should decrease and (2) MODIS α should decrease more sharply than AERONET. Fig 3b shows the plot of Angstrom Exponent against cloud fraction for Terra, Aqua and their associated AERONET measurements. The differences between Terra and Aqua can be explained by calibration differences in the two sensors. There certainly is a decrease of α (increase in particle size) as cloud fraction increases. However, the differences between MODIS and AERONET Angstrom Exponent remain constant for the entire range of cloud fraction. With this consistency it becomes difficult to explain the difference between MODIS and AERONET AOT as simple cloud contamination.

6. Cloud contamination vs. aerosol growth

To understand the relationships between MODIS and AERONET optical thickness and Angstrom Exponent we need to address the fundamental problem of how to differentiate between cloud contamination and variability of the aerosol optical thickness due to aerosol growth by cloud processes and humidification. The AERONET and MODIS cloud screening algorithms may separate cloud contamination from cloud growth differently. Are the differences in Fig. 3 due to stronger cloud contamination of the MODIS retrievals or more allowance for aerosol growth? We use the AERONET data to study this issue.

The main tool for AERONET cloud screening [46] is rejection of AOT variability in two time scales: fast variability of the AOT in between the three measurements taken 30 seconds apart (triplets) at each wavelength separately, and slower variability among measurements taken 15 minutes apart. The fast variability is the main criteria. The algorithm requires that the difference between the maximum and minimum aerosol optical thickness among the triplet measurements is smaller than 0.02 for every wavelength. For high optical thicknesses (AOT>0.7) the threshold is 0.03τ. This algorithm is applied globally to all aerosol types. For the purpose of this study we design a modified cloud screening algorithm, that applies to pollution or smoke aerosol only, by taking advantage of their strong spectral dependence, and quantifies cloud contamination and aerosol growth effects.

Assuming that the cloud optical depth is wavelength independent and that the aerosol optical depth has a wavelength dependence, we can calculate the contribution of cloud contamination to variations in the aerosol field separately from variations of the "true" aerosol. The measured spectral AOT, τ_λ, with possible cloud contamination can be written as:

$$\tau_\lambda = \langle\tau_\lambda\rangle + \Delta\tau_\lambda \qquad (2)$$

where $\Delta\tau_\lambda$ is the variability between the triplet measurements or the 15 minute measurements of the aerosol optical thickness, and $<\tau_\lambda>$ is the spectral AOT of the bulk of the aerosol.

The cloud contamination is the difference between the measured aerosol variability at 0.87 μm and the variability that corresponds to the bulk aerosol spectral dependence:

$$\Delta\tau_{cloud} = [\Delta\tau_{0.87} - \Delta\tau_{0.44}(<\tau_{0.87}>/<\tau_{0.44}>)] \quad (3)$$

restricted for Angstrom exponent > 0.2. $\Delta\tau_{cloud}$ is the residual spectrally neutral variability of the AOT measurements. What Eq. 3 represents is that if the spectral dependence of $\Delta\tau_\lambda$ is similar to that of $<\tau_\lambda>$ then the measurement is not cloud contaminated for any magnitude of the variability $\Delta\tau_\lambda$. In such case $\Delta\tau_{cloud} = 0$.

The new proposed cloud screening allows aerosol variability not to be rejected as cloud, as long as it has similar spectral properties to the bulk of the aerosol. However, aerosol growth can also reduce the aerosol wavelength dependence and generate a positive $\Delta\tau_{cloud}$. Analysis of sunphotometer data in the Eastern US humid and polluted summer environment [48] showed that changes in the relative humidity can change the Angstrom exponent by up to 0.2, corresponding to $\Delta\tau_{cloud}/\tau_{aerosol}$=20%. Therefore cloud contamination needs to be defined above a given threshold of $\Delta\tau_{cloud}$:

$$\Delta\tau_{cloud} > n + h\tau_{aerosol} \qquad \text{for } 0.55\ \mu\text{m} \quad (4)$$

In Fig. 4 we compare the AERONET original cloud screening with the new concept for n=0.005 and h=0.02 or 0.05, for measurements in Lille, France during September 2004. The value of "n" means that we allow for noise in the data of $\Delta\tau$<n not to be called a cloud, and "h" means that we allow variability of 100h% in the wavelength independent component of the AOT to be associated with aerosol growth rather than cloud contamination. In Fig. 4 we also show the cloud screened level 1.5 AERONET AOT data and application of the new algorithm to the level 1.0 data. The new algorithm included additional points in the variable portion of the day. On average for the month of September the new algorithm had 15% additional points for h=0.02 and 44% more points for h=0.05, both possible result of aerosol growth. The corresponding change in the monthly average of AOT and Angstrom exponent (at 0.67 μm) is from (0.145 & 1.22) for the AERONET algorithm to (0.170 & 1.32) For h=0.02 and (0.174 & 1.28) For h=0.05. Note that the new algorithm, while adding data, also increased the Angstrom exponent, by screening small residual clouds with a finer threshold. Therefore differences in the AOT of ~ 0.02±0.01 between MODIS and AERONET (from Fig. 3) as a function of the cloud fraction can be equally associated with aerosol growth as with cloud contamination. However application of the new algorithm to dust and dust mixed with smoke or pollution is more complex and beyond the scope of the present paper.

7. The effect of the diurnal cycle

The MODIS observations take place at a narrow interval of the diurnal cycle, where Terra crosses the equator southward about 10:30 local solar time, whereas Aqua crosses northward about 13:30. Because of the difference in direction, midlatitude time differences between Terra and Aqua are approximately 1.5 hours in the Northern Hemisphere and 4.5 hours in the Southern. The use of MODIS data to represent regional aerosol burden, requires understanding of the diurnal representation of these two times of the day. A previous analysis of AERONET data [49] found that there is no statistically significant difference between the AOT monthly averages, whether they were taken only around 10:30 or 1:30, or averaged throughout the day, although a diurnal cycle can exist [50] near aerosol sources that have a strong diurnal cycle like smoke from fires, both prescribed fires in the tropics that are lit in the afternoon and wild fires that emits more during the day in the presence of strong winds. Over the oceans, far from aerosol sources, [51], we would expect that either Terra or Aqua aerosol measurements would be representative of the daily averaged AERONET AOT [49].

In Fig. 5 we test the validity of this hypothesis using the actual MODIS data from Terra and Aqua on a 1° latitude and longitude resolution, over several AERONET stations in oceanic regions. The monthly average value was calculated if there were at least 5 days of reported data for each instrument. These are not collocated data, meaning that the AERONET data contain information from all daylight hours, not just at the time of overpass. Note the possibility, that in high cloudy conditions, data observed by AERONET, Terra and Aqua are taken from different days of the month.

The plots in Fig. 5 distinguish among 4 aerosol types: dust, smoke, marine and urban aerosol, based on their location/season. The average differences between the MODIS measurements and AERONET are also given in Table 1, for all available AERONET oceanic data during one year in 2002-2003 (Level 2.0 data). On average Terra and Aqua AOTs are higher from AERONET by 0.01 ± 0.005. Thus, despite different sampling strategies, MODIS can represent AERONET's long-term statistics to within the measurement uncertainties of both instruments.

However, there are differences for both small and large optical thickness conditions. For optical thickness $\tau < 0.2$ the difference is $\Delta\tau \sim 0.02$ both for Terra and Aqua. However, for high AOTs the MODIS results are lower for smoke and pollution, apparently due to higher aerosol absorption [52,53], than that assumed in the MODIS inversion process. For dust the AOT is slightly higher probably due to the effect of dust nonsphericity that is not included presently in the aerosol algorithm. Depending on the scattering angles in the data set nonsphericity can increase or decrease the dust AOT.

In Fig. 6 the comparison of Terra, Aqua and AERONET measurements is shown for 8 stations as a function of the month. Differences between Terra and Aqua can either indicate strong diurnal cycle or low density of data. Nes-Ziona in Israel and COVE in the Eastern US represent locations influenced with pollution aerosols. Stations influenced by desert dust (Capo Verde and Dakhla) show very good agreement between the measurements, except during the summer months at Capo Verde where Terra and Aqua report higher values. Tahiti and Ascension Island are both remote ocean sites, however

the agreement in Tahiti is better than that in Ascension Island where the satellite data rate are lower in Dec.-March. It is during this period when biomass burning from Africa affects Ascension Island. Very good agreement is observed over Rome.

8. Glint and scattering angles

The validation data set that was used to observe the effect of cloud on the MODIS aerosol measurements can be also used to observe the effect of the different glint and scattering angles on the measurements. In Fig. 7 we plot the average error in the AOT measurements from MODIS on Terra and Aqua and the average of the absolute errors as a function of the glint angle and separately as a function of the scattering angle. The results show, that the glint angle, on average has no significant effect on the accuracy. The errors tend to be higher, and therefore the average of the absolute errors higher as we approach the glint for glint angle <50°. The dependence on the scattering angle shows also little dependence with some improvement of the accuracy for scattering angles <110° as suggested by Chylek et al., [54], though the density of the data for small scattering angles is very low. The errors are also lower around scattering angle of 160° may be due to lower impact of aerosol nonsphericity.

9. Implications to the use of the MODIS aerosol data

The accuracy of the MODIS aerosol data has different implications depending on the application for which they are used. MODIS estimates of regional and global average aerosol optical thicknesses are sensitive to cloud contamination. For 2001-2003 the MODIS average AOT over the ocean [35] weighted by the cloud free area, is ~0.13±0.01 (the unweighted value is 0.14), while several chemical transport models [55-57] estimate 0.090±0.005, where 0.005 is the deviation among the three models. The present analysis shows cloud contamination of 0.015±0.003 for cirrus. The difference between MODIS measurements and AERONET shows dependence of the AOT on the cloud fraction that may indicate additional cloud contamination of AOT of $\Delta\tau$~0.01±0.005 or can indicate different sampling of the effects of aerosol growth by the two algorithms. Therefore, the total cloud contamination is estimated to be at most 0.025±0.005, with a more likely estimate closer to 0.020 after accounting for the probability of aerosol growth issues. This reduces the difference between the MODIS global measurements over the oceans and the transport models from 0.04-0.05 to ~0.02.

Another range of applications is the observations of aerosol influence on other atmospheric constituents, e.g. on the cloud microphysics and cloud development [29,58,59]. In such studies the cloud parameter is plotted as a function of the AOT, assuming that the change in the AOT represents the true increase in the aerosol load. In Fig. 3 we analyzed the dependence of possible cloud contamination on the cloud fraction. For example, an increase in cloud fraction of 0.25 can cause a maximum increase in the observed AOT of 0.01, independent of the values of the AOT.

Here we test this conclusion by using an additional measure of aerosol derived by MODIS, namely the change in the Ångström Exponent as a function of the AOT. Cloud

contamination is expected to have neutral spectral reflectance due to the large size of cloud droplets, thus reducing the Angstrom exponent. If cloud contamination is an important factor in variation of the aerosol AOT, than we can expect the Ångström Exponent to decline as a function of the increase in AOT. In Fig. 8 we plot the Ångström Exponent and the cloud fraction as a function of the AOT, for 3 latitude zones of the Atlantic Ocean analyzed for June-Aug 2002. Each point represents average on 50 daily values, with similar AOT in 1° resolution. This analysis differs from the previous analysis in Section 5 and Figure 3b in that the previous analysis was confined to points collocated with AERONET stations, and here we use all available mid-ocean data of the Atlantic basin for the period indicated. Before we were looking for discrepancies from AERONET as cloudiness increased. Here we are looking for relationships between aerosol size and aerosol optical thickness. In all cases for AOT<0.3, as AOT increases the Ångström Exponent increases or remains constant (for dust). The increase is due to transition from pure marine aerosol with Ångström Exponent around 0.3 to smoke, or pollution with Ångström Exponent of 1.0 or higher. Therefore the increase of AOT cannot be explained by increase of cloud contamination or contamination from illumination from clouds sides. For the pollution zone (30°-60°N) for AOT>0.3 the Ångström Exponent decreases. However the cloud fraction is constant or decreases also, therefore this cannot be explained by cloud contamination but rather aerosol growth.

10. Conclusions

We found a residual cloud contamination, in particular very thin cirrus on the MODIS aerosol optical thickness (AOT), despite the MODIS unique cirrus detection channel, and vigorous spatial-spectral cloud rejection. Unresolved cirrus contributes 0.015±0.003 to the global aerosol average aerosol optical thickness (AOT) over cloud free oceans. An additional 0.010±0.005 of excess optical thickness is associated with cloudy conditions, however it is difficult to distinguish with present data between broken cloud contamination and aerosol growth. Though the total contamination of 0.020±0.005 is essential in using the satellite data to evaluate aerosol simulated by global chemical transport models, it is not detrimental in addressing aerosol effect on cloud microphysics, albedo and precipitation. We also found the aerosol to show overall a weak diurnal cycle, though a strong diurnal cycle is expected in the vicinity of sources with a strong diurnal variability.

Acknowledgement

Part of the work was performed while Y.J. Kaufman was a visiting professor in the Laboratory for Atmospheric Optics directed by D. Tanré. NASA and CNES funded the MODIS and AERONET data used in the study. We also want to thank J. Coakley from Oregon State University for provocative questions that stimulated some of the analysis.

References:

1. King, M. D., W. P. Menzel, Y. J. Kaufman, D. Tanré, B. C. Gao, S. Platnick, S. A. Ackerman, L. A. Remer, R. Pincus, and P. A. Hubanks, 2003: Cloud and aerosol

properties, precipitable water, and profiles of temperature and humidity from MODIS. *IEEE Trans. Geosci. Remote Sens.*, 41, 442-458.
2. Remer, L.A., Y. J. Kaufman, D. Tanre, et al., The MODIS Aerosol Algorithm, Products and Validation, J. Atmos. Sci.,62 (4),947-973, 2005
3. Barnaba F, Gobbi GP, Aerosol seasonal variability over the Mediterranean region and relative impact of maritime, continental and Saharan dust particles over the basin from MODIS data in the year 2001, Atmos. Chem. & Phys. 4: 2367-2391 NOV 30 2004.
4. Bremer H, Kar J, Drummond JR, et al., Spatial and temporal variation of MOPITT CO in Africa and South America: A comparison with SHADOZ ozone and MODIS aerosol, J. Geoph. Res., 109 (D12): Art. No. D12304 JUN 22 2004
5. Chin M, Chu A, Levy R, et al., Aerosol distribution in the Northern Hemisphere during ACE-Asia: Results from global model, satellite observations, and Sun photometer measurements, J. Geoph. Res, 109 (D23): Art. No. D23S90 DEC 2 2004
6. Damoah R, Spichtinger N, Forster C, et al., Around the world in 17 days - hemispheric-scale transport of forest fire smoke from Russia in May 2003, Atmos. Chem. & Phys.4: 1311-1321 AUG 23 2004
7. Edwards DP, Emmons LK, Hauglustaine DA, et al., Observations of carbon monoxide and aerosols from the Terra satellite: Northern Hemisphere variability, J. Geoph. Res., 109 (D24): Art. No. D24202 DEC 16 2004
8. Geogdzhayev IV, Mishchenko MI, Liu L, et al., Global two-channel AVHRR aerosol climatology: effects of stratospheric aerosols and preliminary comparisons with MODIS and MISR retrievals, J. Quant. Spect. & Rad. Trans. 88 (1-3): 47-59 SEP 15 2004
9. Ichoku C, Kaufman YJ, Remer LA, et al., Global aerosol remote sensing from MODIS, Advanc. Space Res. 34 (4): 820-827, 2004
10. Matsui T, Kreidenweis SM, Pielke RA, et al., Regional comparison and assimilation of GOCART and MODIS aerosol optical depth across the eastern US, Geoph. Res. Let. 31 (21): Art. No. L21101 NOV 2 2004
11. Reid JS, Prins EM, Westphal DL, et al., Real-time monitoring of South American smoke particle emissions and transport using a coupled remote sensing/box-model approach, Geoph. Res. Let., 31 (6): Art. No. L06107 MAR 18 2004
12. Roskovensky JK, Liou KN, Garrett TJ, et al., Simultaneous retrieval of aerosol and thin cirrus optical depths using MODIS airborne simulator data during CRYSTAL-FACE and CLAMS, Geoph. Res. Let. 31 31 (18): Art. No. L18110 SEP 23 2004
13. Vachon F, Royer A, Aube M, et al., Remote sensing of aerosols over North American land surfaces from POLDER and MODIS measurements, Atmos. Environ. 38 (21): 3501-3515 JUL 2004
14. Wooster MJ, Zhang YH, Boreal forest fires burn less intensely in Russia than in North America, , Geoph. Res. Let. 31 (20): Art. No. L20505 OCT 26 2004
15. Xia XA, Chen HB, Wang PC, Validation of MODIS aerosol retrievals and evaluation of potential cloud contamination in East Asia, J. Env. Scie.-China 16 (5): 832-837 2004
16. Engel-Cox JA, Holloman CH, Coutant BW, et al., Qualitative and quantitative evaluation of MODIS satellite sensor data for regional and urban scale air quality, Atmos. Environ., 38 (16): 2495-2509 MAY 2004

17. Hutchison KD, Smith S, Faruqui S, The use of MODIS data and aerosol products for air quality prediction, Atmos. Env., 38 (30): 5057-5070 SEP 2004
18. Zheng YG, Zhu PJ, Chan CY, et al., Influence of biomass burning in Southeast Asia on the lower tropospheric ozone distribution over South China, Chinese J. Geoph.-Chinese Ed. 47 (5): 767-775 SEP 2004
19. Christopher SA, Zhang JL, Cloud-free shortwave aerosol radiative effect over oceans: Strategies for identifying anthropogenic forcing from Terra satellite measurements, Geoph. Res. Let. 31 31 (18): Art. No. L18101 SEP 16 2004
20. Li F, Vogelmann AM, Ramanathan V, Saharan dust aerosol radiative forcing measured from space, J. Clim. 17 (13): 2558-2571 JUL 2004
21. Menon S, Current uncertainties inassessing aerosol effects on climate, ANNUAL Rev. Environ. Resources, 29: 1-30 2004
22. Ramana MV, Ramanathan V, Podgorny IA, et al., The direct observations of large aerosol radiative forcing in the Himalayan region, Geoph. Res. Let., 31 (5): Art. No. L05111 MAR 6 2004
23. Vinoj V, Babu SS, Satheesh SK, et al., Radiative forcing by aerosols over the Bay of Bengal region derived from shipborne, island-based, and satellite (Moderate-Resolution Imaging Spectroradiometer) observations J. Geoph. Res., 109 (D5): Art. No. D05203 MAR 12 2004
24. Yu HB, Dickinson RE, Chin M, et al., Direct radiative effect of aerosols as determined from a combination of MODIS retrievals and GOCART simulations, J. Geoph. Res 109, (D3): Art. No. D03206 FEB 12 2004
25. Haywood JM, Osborne SR, Abel SJ, The effect of overlying absorbing aerosol layers on remote sensing retrievals of cloud effective radius and cloud optical depth, Quart. J. Royal Meteor. Soc. 130 (598): 779-800 Part A APR 2004
26. Pierangelo C, Chedin A, Heilliette S, et al., Dust altitude and infrared optical depth from AIRS, Atmos. Chem. & Phys. 4: 1813-1822 SEP 13 2004
27. Slater JF, Dibb JE, Campbell JW, et al., Physical and chemical properties of surface and column aerosols at a rural New England site during MODIS overpass, Rem. Sens. Environ. 92 (2): 173-180 AUG 15 2004
28. Sumanth E, Mallikarjuna K, Stephen J, et al., Measurements of aerosol optical depths and black carbon over Bay of Bengal during post-monsoon season, Geoph. Res. Let., 31 (16): Art. No. L16115 AUG 26 2004
29. Koren I, Kaufman YJ, Direct wind measurements of Saharan dust events from Terra and Aqua satellites, Geoph. Res. Let., 31 (6): Art. No. L06122 MAR 25 2004
30. Koren I, Kaufman YJ, Remer LA, et al., Measurement of the effect of Amazon smoke on inhibition of cloud formation, Science, 303 (5662): 1342-1345 FEB 27 2004
31. Holben BN, Tanre D, Smirnov A, et al., An emerging ground-based aerosol climatology: Aerosol optical depth from AERONET, *J. Geophys. Res,* **106**, 12067-12097, 2001
32. Remer, L. A., D. Tanré, Y. J. Kaufman, et al., Validation of MODIS aerosol retrieval over ocean. Geophys. Res. Lett., 29 (12): art. no. 1618 JUN 15 2002
33. Tanré, D., Y. J. Kaufman, M. Herman and S. Mattoo, Remote sensing of aerosol over oceans from EOS-MODIS., J. Geophys. Res, 102, 16971-16988, 1997
34. Levy, R C., L. A. Remer, D. Tanré, Y. J. Kaufman, C. Ichoku, B. N. Holben, J. M. Livingston, P. B. Russell, H. Maring, Evaluation of the MODIS retrievals of dust aerosol over the ocean during PRIDE, *J. Geophys. Res.*Vol. 108, No. D19, 8594,

10.1029/2002JD002460, 23 July 2003
35. Remer, L.A. and Y. J. Kaufman, Aerosol effect on the distribution of solar radiation over the global oceans derived from five years of MODIS retrievals, Atmos. Chem. Phys.
36. Kaufman, Y.J., B. N. Holben, S. Mattoo, D. Tanré, L.A. Remer, T. Eck and J. Vaughn: Aerosol radiative impact on spectral solar flux reaching the surface, derived from AERONET principal plane measurements, J. Atmos. Scie., 59, 633-644, 2002.
37. Martins, J. V., D. Tanré, L.A. Remer, et al.,, MODIS Cloud screening for remote sensing of aerosol over oceans using spatial variability, Geophys. Res. Lett., 29(12),10.1029/2001GL013252, 2002.
38. Gao B.-C., Y.J. Kaufman, D. Tanré and R.-R. Li, Distinguishing tropospheric aerosol from thin cirrus clouds for improved aerosol retrievals using the ratio of 1.37 μm and 1.24 μm channels. Geophys. Res. Lett.. 29 (18): art. no. 1890 SEP 15 2002
39. Brennan, J. I., Y. J. Kaufman, I. Koren and R. R. Li, Aerosol-cloud interaction – misclassification of MODIS clouds in heavy aerosol, IEEE TGRS, 43, 911-915 APR 2005
40. Ichoku, C., D. A. Chu, S. Mattoo , et al., A Spatio-Temporal Approach for Global Validation and Analysis of MODIS Aerosol Products,. Geophys. Res. Lett., 29 (12): art. no. 1616 JUN 15 2002
41. Anderson T.L., Charlson RJ, Winker DM, et al., *J. Atmos. Scie*. 60 (1): 119-136 JAN 2004
42. Ichoku, C., L. A. Remer, and T. F. Eck (2005), Quantitative evaluation and intercomparison of morning and afternoon Moderate Resolution Imaging Spectroradiometer (MODIS) aerosol measurements from Terra and Aqua, J. Geophys. Res., 110, D10S03, doi:10.1029/2004JD004987.
43. Eck, T.F., B.N. Holben, J.S. Reid, O. Dubovik, A. Smirnov, N.T. O'Neill, I. Slutsker, and S. Kinne, Wavelength dependence of the optical depth of biomass burning, urban and desert dust aerosols, *J. Geophys. Res.,* **104**, 31333-31349, 1999.
44. Wen G., R.F. Cahalan, S. Tsay and L. Oreopoulos, Impact of cumulus cloud spacing on Landsat atmospheric corrections and aerosol retrievals, *J. Geophys. Res.,* **106**, 12129-12138, 2001.
45. Gao, B.-C. and Y. J. Kaufman, 1996: Selection of the 1.375 μm MODIS channel for remote sensing of cirrus clouds and stratospheric aerosols from space. *J.Atmos. Sci,* 52, 4231-4237.
46. Smirnov A., B. N. Holben, T. F. Eck, et al., 2000: Cloud screening and quality control algorithms for the AERONET database, *Rem. Sens. Env.*, **73**, 337-34
47. Kinne, S., T.P. Ackerman, M. Shiobara, A. Uchiyama, A.J. Heymsfield, L. Miloshevich, J. Wendell, E.W. Eloranta, C. Purgold, and R.W. Bergstrom, Cirrus cloud radiative and microphysical properties from ground observations and in situ maesurements during FIRE 1991 and their application to exhibit problems in cirrus solar radiative transfer modeling, J. Atmos. Sci., 54, 2320-2344, 1997.
48. Kaufman, Y. J. and R. S. Fraser, 1983: Light Extinction by Aerosol During Summer Air Pollution. *J. Appl. Meteor*., 22, 1694-1706.
49. Kaufman, Y.J., B. N. Holben, D. Tanré, et al., Will aerosol measurements from Terra and Aqua polar orbiting satellites represent the daily aerosol abundance and properties? Geoph. Res. Let., 27, 3861-3864, 2000.

50. Smirnov, A., B.N.Holben, T.F.Eck, I.Slutsker, B.Chatenet, and R.T.Pinker, Diurnal variability of aerosol optical depth observed at AERONET (Aerosol Robotic Network) sites, Geophys. Res. Lett. , 29 (23), 2115, doi:10.1029/2002GL016305, 2002.
51. Smirnov, A., B.N.Holben, Y.J.Kaufman, et al., Optical properties of atmospheric aerosol in maritime environments. *J. Atmos. Sci,* **59**, 501-523, 2002
52. Ichoku, C., L. A. Remer, Y. J. Kaufman, R. Levy, D. A. Chu, D. Tanré, and B. N. Holben, MODIS observation of aerosols and estimation of aerosol radiative forcing over southern Africa during SAFARI 2000, J. Geophys. Res., 108 (D13), 8499, doi:10.1029/2002JD002366, 2003.
53. Dubovik, O., B.N. Holben, T. F. Eck, et al., Climatology of aerosol absorption and optical properties in key worldwide locations, *J. Atmos. Sci,* **59**, 590-608, 2002
54. Chylek P, Henderson B, Mishchenko M, Aerosol radiative forcing and the accuracy of satellite aerosol optical depth retrieval, *J. Geophys. Res.*, 108 (D24): Art. No. 4764 DEC 18 2003
55. Chin, M *et al.*, Tropospheric aerosol optical thickness from the GOCART model and comparisons with satellite and Sun photometer measurements, *J. Atmos. Sci.,* 59, 461-483, 2002.
56. Reddy, M. S., O. Boucher, N. Bellouin, et al., Global multi-component aerosol optical depths and radiative forcing estimates in the LMDZT general circulation model, *J. Geophys. Res.*, 110 (D10): Art. No. D10S16 APR 21 2005.
57. Takemura, T, Nakajima T, Dubovik O, et al., Single-scattering albedo and radiative forcing of various aerosol species with a global three-dimensional model, J. Climate, 15, 333-352 2002
58. Kaufman, Y. J., I. Koren, L. A. Remer, D. Rosenfeld and Y. Rudich, Smoke, Dust and Pollution Aerosol Clouding the Atlantic Atmosphere, submitted to PNAS
59. Koren, I. Y. J. Kaufman, L. A. Remer, D. Rosenfeld and Y. Rudich Aerosol impact on the development and coverage of Convective clouds for submitted to Nature

Table 1: Comparison of Terra and Aqua aerosol optical thicknesses at 550 nm to AERONET for all oceanic station during one year 2002-2003. Each dataset over each station is averaged monthly independent of each other. The data are then sorted by the AERONET AOT and averaged in groups of 8-30. Systematic deviations in the diurnal cycle would affect the difference between the satellite and AERONET data.

Aeronet	Terra	Terra-Aeronet	Aqua	Aqua-Aeronet
0.054±0.01	0.097±0.05	0.043	0.080±0.03	0.025
0.086±0.01	0.109±0.03	0.023	0.107±0.03	0.021
0.123±0.01	0.153±0.06	0.031	0.147±0.04	0.024
0.172±0.01	0.187±0.05	0.016	0.192±0.08	0.021
0.241±0.03	0.242±0.07	0.000	0.248±0.11	0.007
0.354±0.03	0.344±0.10	-0.010	0.322±0.08	-0.032
0.481±0.05	0.480±0.11	-0.001	0.438±0.12	-0.043
0.641±0.10	0.590±0.21	-0.051	0.550±0.21	-0.091
All: 0.208	**0.223**	**0.015**	**0.215**	**0.007**

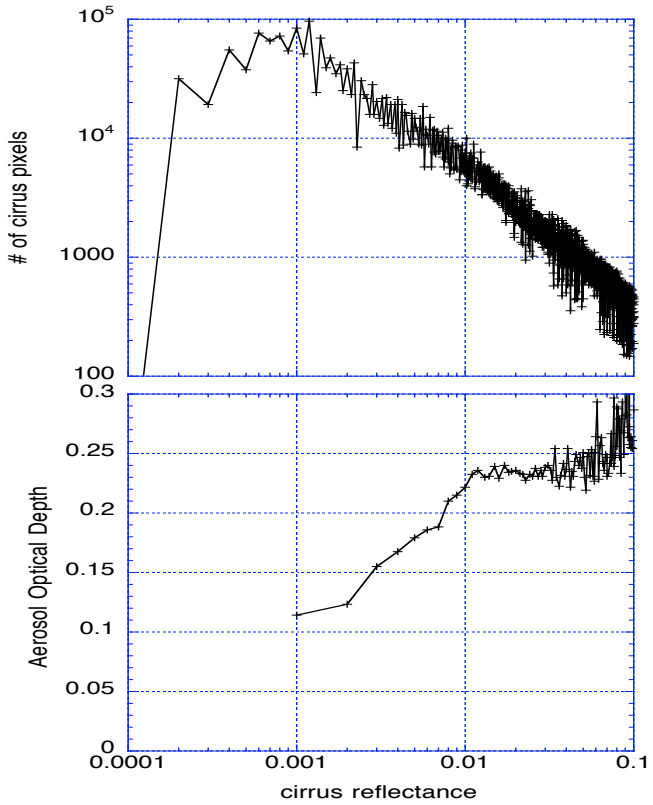

Fig 1: Example of the analysis of cirrus contamination. Top: histogram of the cirrus reflectance measured by MODIS over the globe for one day (April 1st 2004). Each point is the average over a 10 km grid box. Note the logarithmic scale. Bottom: Average aerosol optical thickness (AOT) as a function of a given range of cirrus reflectance (i.e. first point is the average AOT for cirrus reflectance of 0-0.001, second for 0.001-0.002 etc.) Cirrus contamination is measured as the elevation of the AOT above its value for the lowest cirrus reflectance interval.

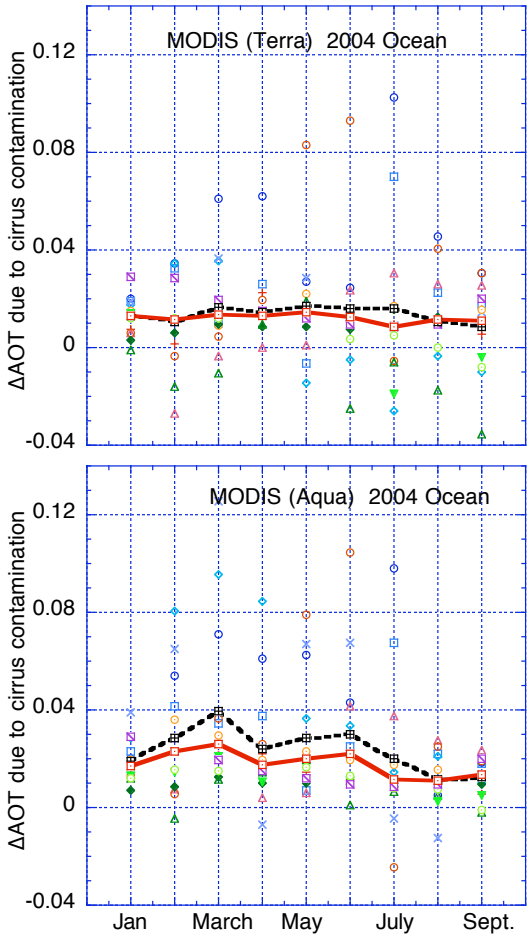

Fig 2: Plot of the cirrus contamination calculated using scatter plots shown in Fig 1. The earth was divided into 13 zones, for each the average contamination over the ocean is plotted by symbols as a function of the month for 2004. The solid line is the median contamination calculated as the average of 25th to 75th percentile among the 13 zones. The dashed line is the simple average. Top is for Terra and bottom for Aqua.

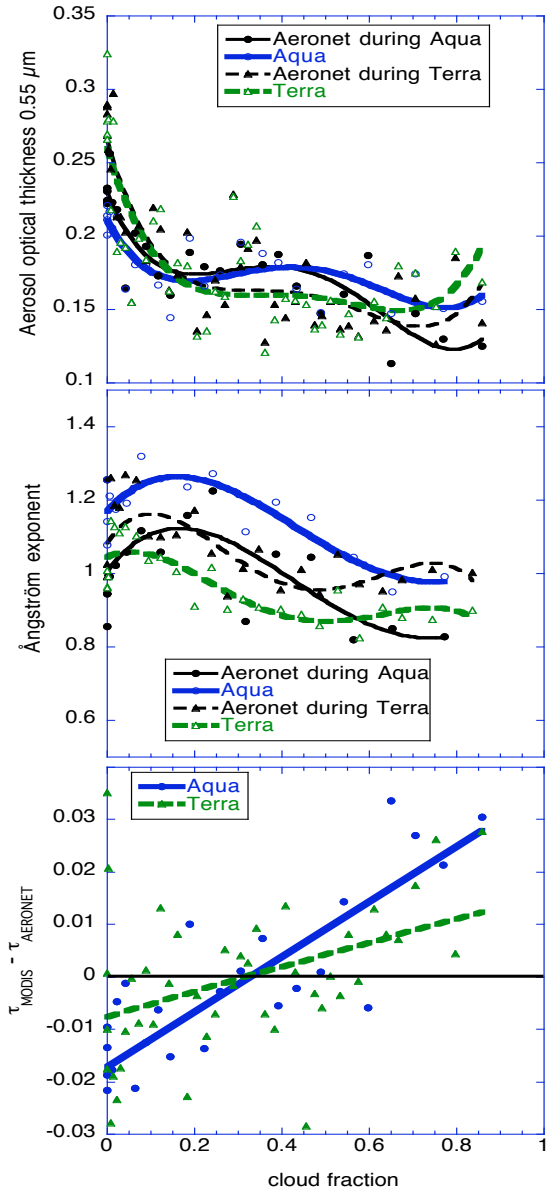

Fig 3. Top: Scatter plot of the MODIS aerosol optical thickness (AOT) over the ocean and the AERONET measured AOT as a function of the cloud fraction at 550 nm. The cloud fraction is defined here as the fraction of the points that were rejected from analysis by the aerosol algorithm. AERONET spectral measurements were interpolated to 550 nm using a parabolic fit in a logarithmic scale [43]. The 3,500 points in the comparison were sorted as a function of the cloud fraction and averaged in groups of 50. Middle: same for the Ångström exponent for AOT≥0.1. Bottom: the difference between the MODIS and AERONET measurements for Terra (green) and Aqua (blue). Data are taken from the MODIS validation over oceanic AERONET sites. The MODIS measurements are within 25 km of each AERONET station and the AERONET data are within 30 minutes of the MODIS observations. The difference in the AOT, representing the error in the MODIS measurements has a systematic dependence on the cloud fraction. The error dependence on the cloud fraction is: $\Delta\tau_{AQUA}$=-0.017+0.052f_C, and $\Delta\tau_{TERRA}$=-0.008+0.023f_C

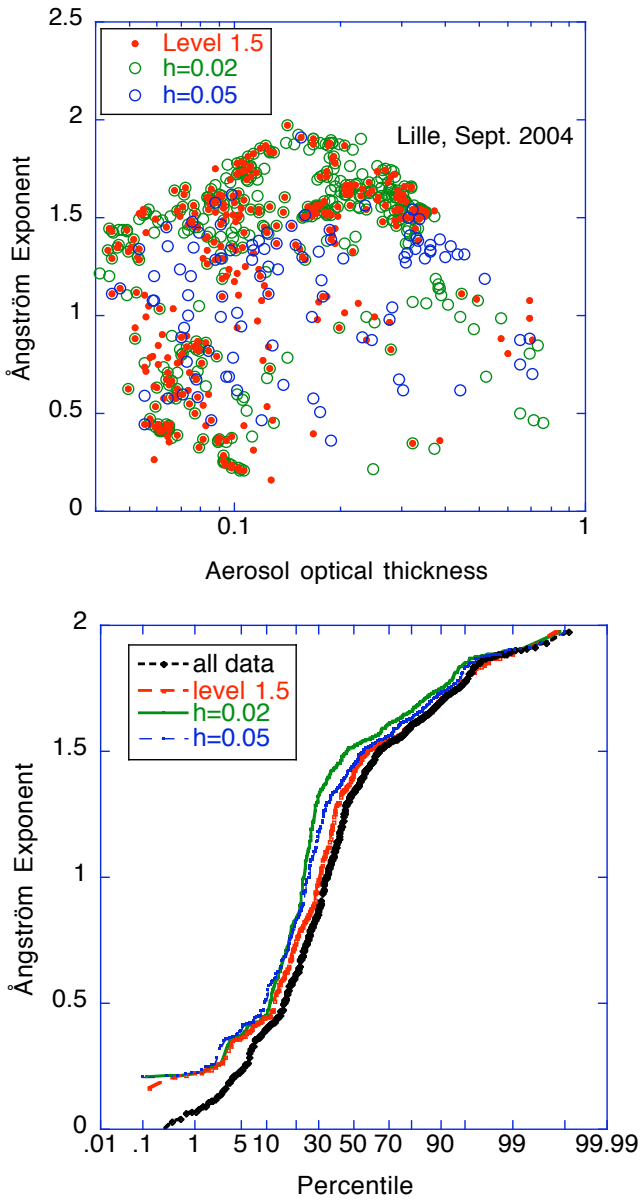

Fig. 4: Comparison of cloud rejection between two algorithms, the AERONET cloud screening (level 1.5 [46]) and a spectral sensitive cloud screening of Eq. 3 for the month of Sept 2004 in Lille. Top: The Ångström exponent as a function of the aerosol optical thickness, for two application of the new algorithm with h=0.02 (green circles), additional points for h=0.05 (blue circles - see Eq. 4), and for the AERONET level 1.5 data (red dots). Bottom: Cumulative histograms of the Angstrom exponent for the new algorithm (green – h=0.02; blue – h=0.05), for the AERONET level 1.5 cloud screened data (red) and for all the level 1.0 (before the level 1.5 cloud screening) data (black).

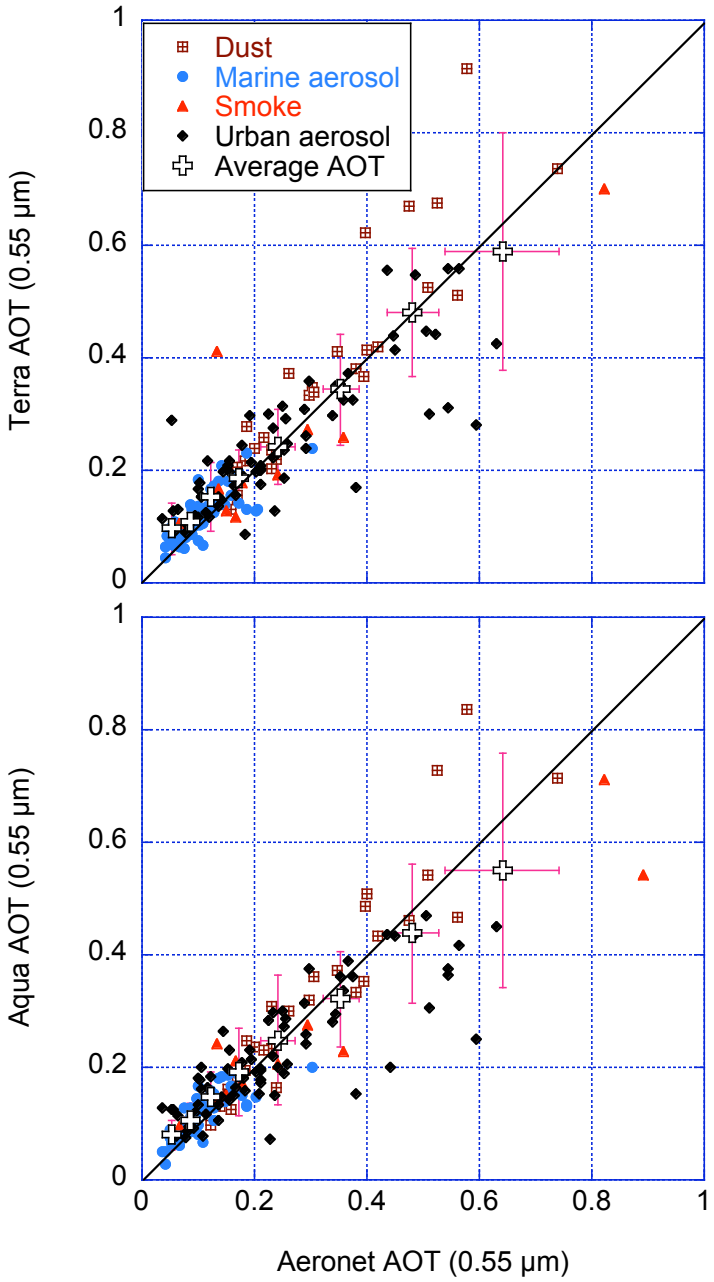

Fig 5: Scatter plot of the monthly independent average of MODIS Terra (top) and Aqua (bottom) aerosol optical thickness (AOT) vs these of AERONET. At least 5 daily measurements were required for each sensor to generate the monthly average. The data are separated into Dust, marine aerosol, smoke and urban aerosol. For each range of the AOT the data are averaged and presented by the + sign with standard deviation. The data are summarized in table 1.

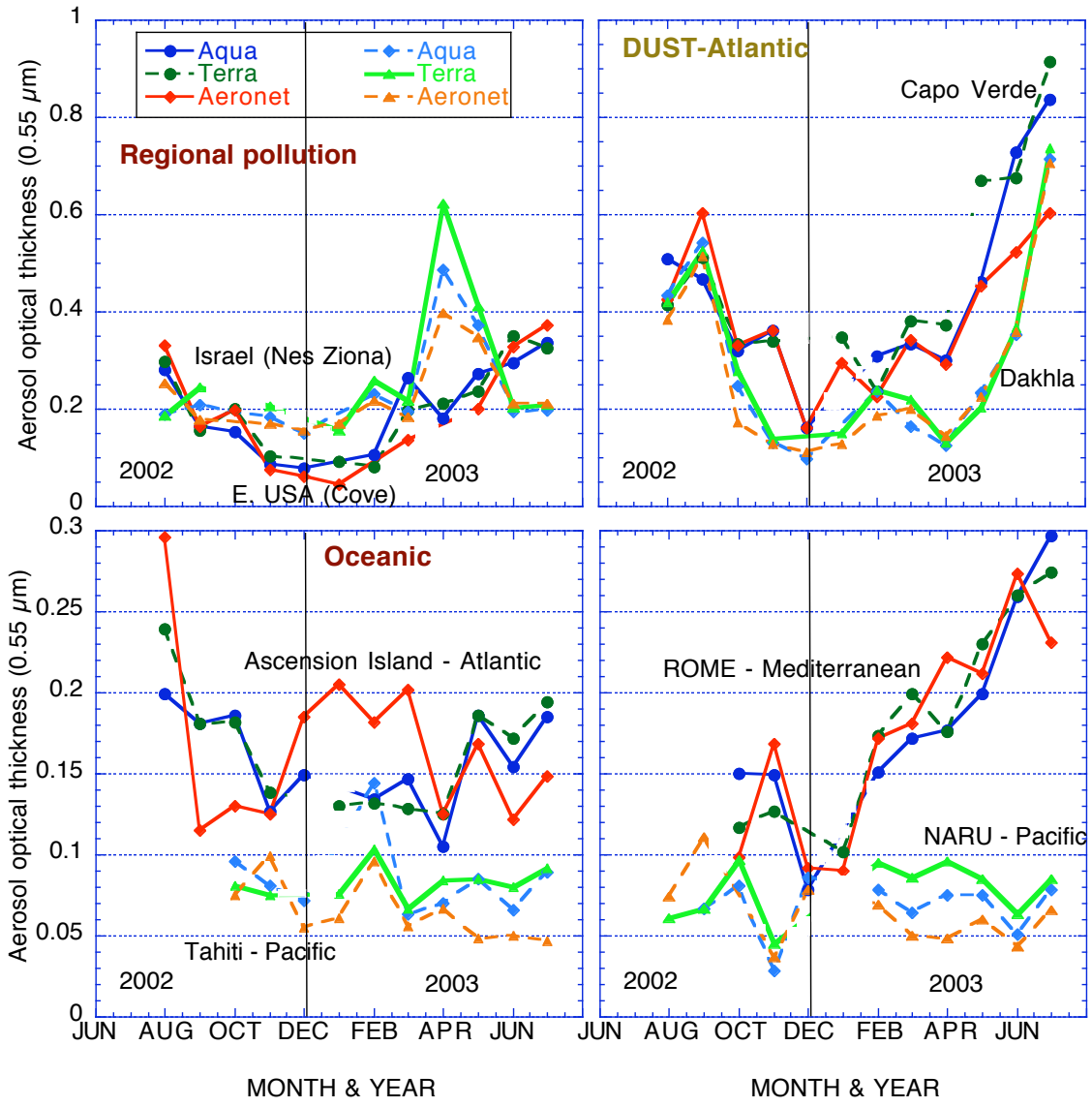

Fig 6: Monthly average aerosol optical thickness values from MODIS Terra (green), Aqua (blue) and AERONET (red and orange), plotted for 8 individual sites as a function of the month of observation. At least 5 measurements were required to generate each monthly average. Months with smaller number of points were skipped.

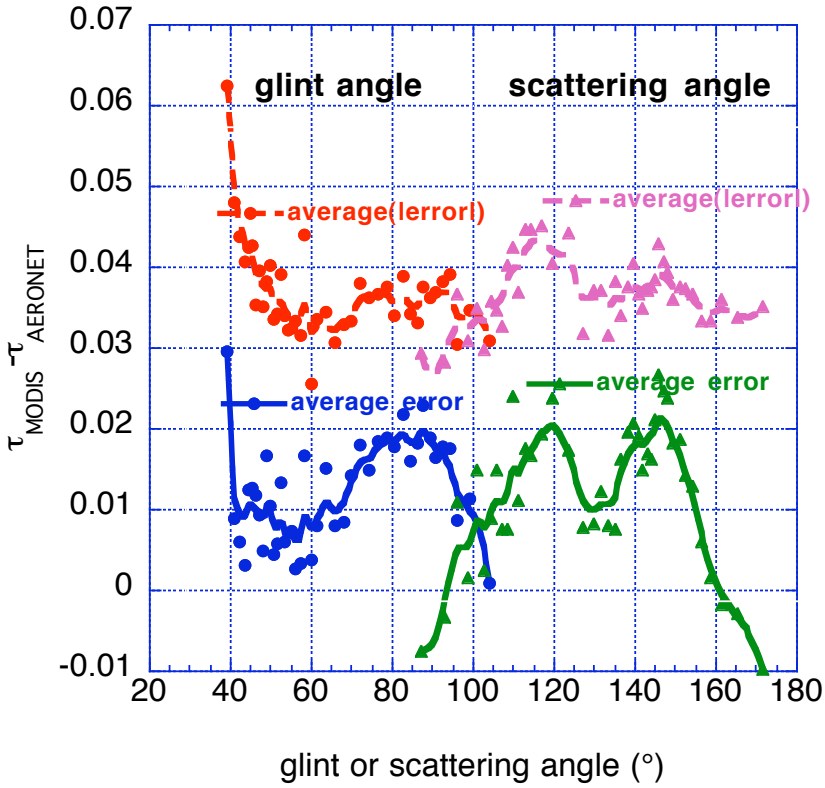

Fig. 7: The average difference between MODIS (Terra and Aqua) and AERONET derived aerosol optical thickness as a function of the glint angle and the scattering angle. The averaging is on 200 points with similar glint or scattering angle. Both averages of the absolute errors (red and pink dashed lines) and of the actual errors (blue and green solid lines) are shown.

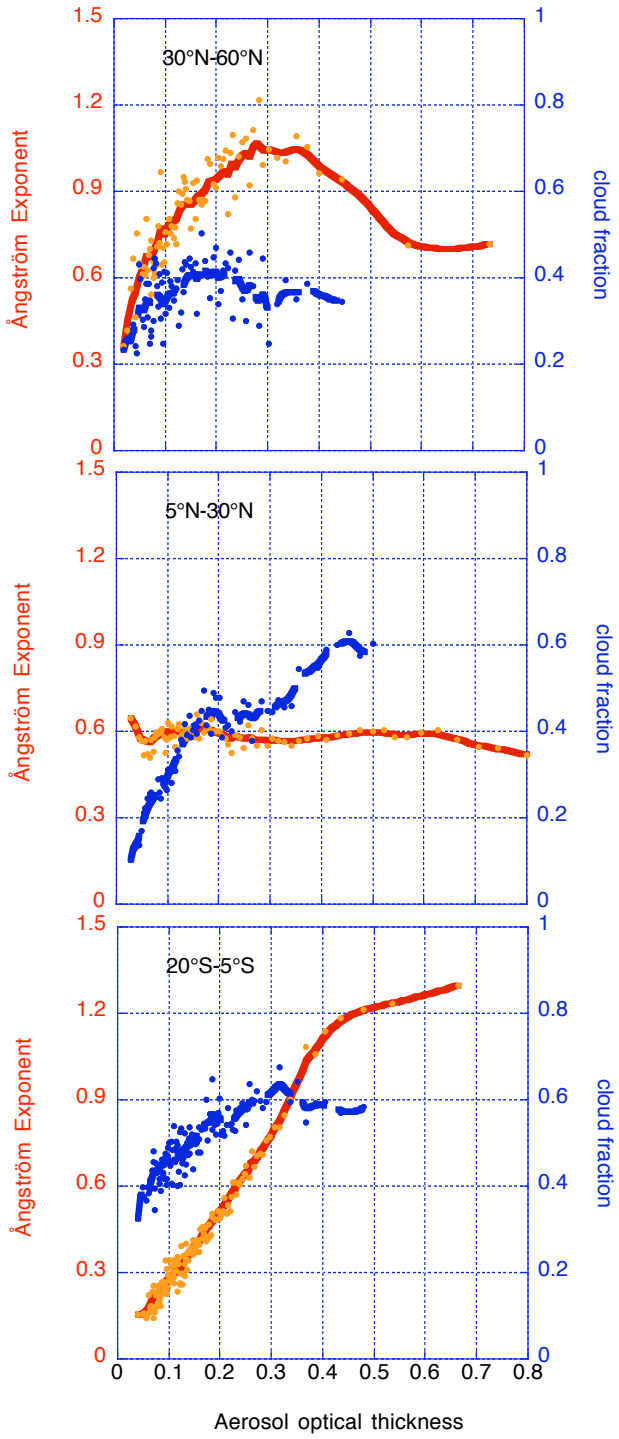

Fig. 8: The aerosol Ångström exponent (a measure of the aerosol size – solid red lines) and cloud fraction (dashed blue line), as a function of the aerosol optical thickness. Cloud fraction is plotted only for AOT<0.5 to avoid effects of aerosol on the cloud fraction [39].